IEEE Access
Multidisciplinary ⋮ Rapid Review ⋮ Open Access Journal

Received April 1, 2021, accepted April 23, 2021, date of publication April 30, 2021, date of current version May 13, 2021.

Digital Object Identifier 10.1109/ACCESS.2021.3076879

Assessing Time-Varying Harmonic Interactions in a Wind Park

VINEETHA RAVINDRAN, (Student Member, IEEE), NASER NAKHODCHI, (Graduate Student Member, IEEE), SARAH RÖNNBERG, (Senior Member, IEEE), AND MATH H. J. BOLLEN, (Fellow, IEEE)

Electrical Power Engineering, Luleå Tekniska Universitet, 931 77 Skellefteå, Sweden

Corresponding author: Vineetha Ravindran (vineetha.ravindran@ltu.se)

This work was supported by the Swedish Energy Agency.

ABSTRACT The harmonic interaction mechanism in a wind park is examined in this paper. The paper investigates the feasibility of a solution to the yet challenging harmonic contribution estimation from multiple sources in a wind park with limited available information, via an extension of a simple modeling approach as well as from detailed analysis of field measurements. The paper has two distinct objectives in assessing harmonic interactions (a) one to extend the classical Norton equivalent model to a multi-measurement wind park system and to suggest potential areas for further model developments from field measurement analysis, and (b) second to draw inferences from field measurements and to develop a new independent concept of analysis from long-term field measurements in the wind park. From practical experience, a new concept of analysis with a 'harmonic interaction break-even point' is introduced. With the help of it, one could identify whether the primary emission (emission from considered source) or secondary emission (emission from a distant source) dominates in the analysis period. In this way, the highest responsibility between different interacting time-varying harmonic sources is evaluated. It was concluded that from long-term measurements one can define a magnitude of power production where a certain harmonic order is canceled or reaches its lowest magnitude. If one finds this cancellation point, one can define a level of secondary/primary emission or at least a feasible range. This knowledge is a step forward towards harmonic contribution analysis.

INDEX TERMS Power quality, wind power generation, power systems harmonics, interharmonics.

I. INTRODUCTION

Harmonic contribution estimation has been studied progressively for years in many systems [1]–[5]. Based on a comparison of different methods for harmonic source identification, it is established that the effectiveness of a method depends on the details of the problem to be addressed [1]. The practicability of these methods is still a question. A benchmark system under steady-state conditions to compare the performance of several proposed methods developed in [2] concludes that in a real system the topology of the grid, linear loads levels, and harmonic generation from non-linear sources may change at any time, so the loads/network responsibility may change with time. It concludes with the need for more realistic studies, especially in distributed energy sources where steady-state operation is occasionally met due to the intermittency in power generation compared to customer load. Such a need is addressed through this work.

In this paper, it is confirmed mathematically that the yet challenging harmonic contribution estimation problem when multiple sources interact together is always under-defined unless exact source impedance values are known. This inference is despite multiple methods stating that the problem can be conditionally solved [3]–[5]. It is proven that even with measurements at multiple locations in a wind park there exists no deterministic solution without additional assumptions or conditions that are seldom met in reality. This is unless there is no information about the individual dynamic turbine impedance as is in most cases.

This paper further investigates how much information one can gain from field measurements for a solution to harmonic contribution estimation with limited information in a wind park. The paper thus contributes to the existing knowledge on harmonic interaction mechanism in a wind park.

The associate editor coordinating the review of this manuscript and approving it for publication was Bin Zhou.

This work is licensed under a Creative Commons Attribution 4.0 License. For more information, see https://creativecommons.org/licenses/by/4.0/

A comparison of harmonic characteristics at the turbine terminal and aggregation point of the wind park at the same time is demonstrated. The individual harmonic characteristics defined by the harmonic interaction mechanism (i.e. time-varying interactions between background emission levels and operating power levels of the turbine) are established through different real scenarios.

Some earlier conclusions regarding the individual harmonic characteristics in a wind park are that the harmonic current magnitude remains unaffected by the operating point of the wind park and individual turbines [6]–[7]. Many existing stochastic and deterministic approaches for the determination of wind park harmonics during planning stages are based on the assumption that the harmonic probability distribution functions do not change with power levels [6]–[8]. In [8], it is stated that the power independent variation of harmonic emission leads to the assumption that they are caused by the grid. In [9], the impact of turbine loading conditions on harmonic emissions is reported to be marginal. A sensitivity of harmonic currents on the operating conditions of the wind park which includes harmonics sourced by the wind park and harmonics sourced by the grid background distortion is established in [10]. It is inferred that it is difficult to distinguish which part of these emissions comes from the summation of wind turbines and which from other sources i.e. grid background harmonics.

In this paper, the terms primary emission and secondary emission as defined in [11] are used to explain field measurements. The primary emission is defined as the emission originating from the considered device. The secondary emission is defined as the emission originating outside of the considered device. It is worth noting that primary emission and secondary emission, therefore, depend on the point of analysis in a system. Every measurement in a wind park is a combination of primary and secondary emissions. It is therefore difficult to identify the exact harmonic sources and quantify them.

From the analysis of field measurements, a 'harmonic interaction break-even point' ($P_{break-even}$) w.r.t active power is introduced. This phenomenon is a result of the interaction between primary and secondary emissions. At the individual turbine terminal, it is the interaction between emissions resulting from turbine operation (primary) and emissions in the background that includes other turbines and upstream grid (secondary). At the aggregation point, i.e. the interface between the park and the public grid, the emission is the result of the interaction between emissions resulting from the wind park as a whole (primary) and emissions in the background from the upstream grid (secondary). $P_{break-even}$ indicates a clear transition of secondary emission dominating over primary emission or vice versa in the individual harmonic characteristics at the individual turbine terminal as well as at the aggregation point. This observation is contrary to the earlier inferences drawn in [7], [12], and [13] that the utility often has the major responsibility for harmonic distortions at the aggregation point.

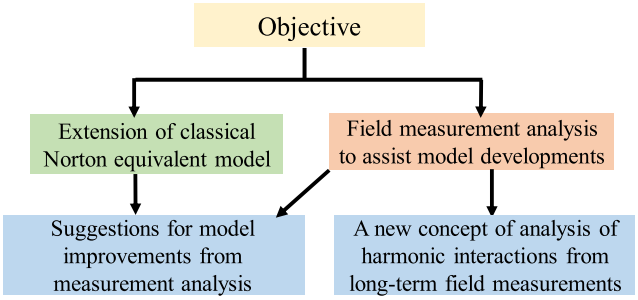

FIGURE 1. Flow chart to represent the objective of the paper.

The objective of this work and the steps involved are represented by the flow chart in Fig. 1. Section II discusses the need to distinguish between primary and secondary emissions. Section III represents the mathematical analysis. Section IV illustrates the results of field measurements. It is worth noting that the terms 'harmonic contribution estimation' and 'distinguish between primary and secondary emissions' are invariably used in this paper and practical inferences are drawn based on the analysis of the considered wind park.

II. NEED TO DISTINGUISH BETWEEN PRIMARY AND SECONDARY EMISSIONS IN A WIND PARK

A three turbine wind park rated at 2 MW in Sweden is considered for this study as shown in Fig. 2. In general, a classical Norton equivalent current source model (representing each DFIG turbine) is recommended for harmonic studies in wind parks due to its simplicity [14]. The field measurements are carried out at the marked locations 'X' in red, which is the secondary side of the transformer to the wind turbines. Three Dranetz Power Explorer PX5, standard power quality monitors were utilized together with voltage and current instrument transformers of sufficient accuracy for the measurements up to a few kHz as per [15]. All current and voltage waveforms were recorded for 200 ms duration in intervals of 30 seconds for 5 months.

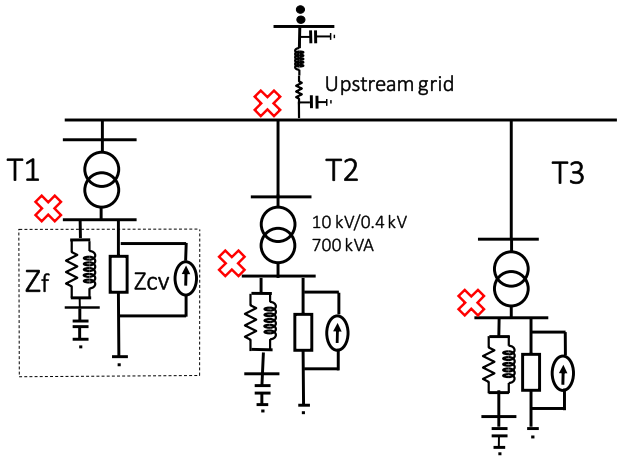

FIGURE 2. Current source model [15] of a three turbine wind park with the upstream grid. T1-T3 are the three wind turbines, Zf represents the high pass filter and Zcv represents the converter impedances respectively.

From practical experience, it was understood that increased waveform distortions are observed with power variations especially at two instances: (a) < 10% of rated power per phase; (b) when maximum power generation is achieved.

The spectrogram in Fig. 3 that is a concatenation of multiple measurements at a turbine terminal shows the time variations in harmonics and interharmonics w.r.t active power. Fig. 3 corresponds to a period where the power production from one turbine occasionally hits the maximum power per phase (222 kW). These observed emissions could be due to an increased converter activity during the same period or due to the influence of secondary emissions from other turbines or upstream grid. An increased converter activity due to a pitch-angle controller that will limit the power when the turbine reaches the nominal power is explained in [16] and this would indicate that this increased emission is due to primary emission. The need to distinguish between primary and secondary emission when multiple sources are interacting at the same time in a wind park can be summarized as:

(a) To understand the relative harmonic contribution of the wind park and the utility (the percent of shared responsibility) at the aggregation point, (b) which source has the highest responsibility to harmonics/interharmonics at the considered point of interest in the analysis period, and (c) to understand the time-varying nature of primary/secondary emissions.

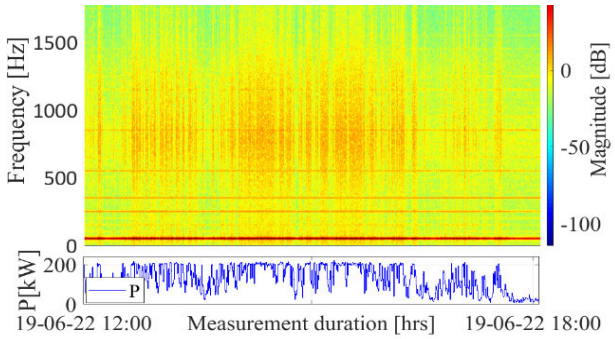

FIGURE 3. Spectrogram showing harmonic and interharmonic variations in current per phase plotted w.r.t power at turbine terminal on a day with max power production attained intermittently.

In Section III, using circuit theory concepts we first perform mathematical analysis to investigate if we can distinguish primary and secondary emission with a deterministic approach and limited information of the wind park.

III. MATHEMATICAL ANALYSIS TO DISTINGUISH BETWEEN PRIMARY AND SECONDARY EMISSION

A Norton equivalent model for harmonics of a single turbine operating together with the grid is considered first as in Fig. 4. The measured harmonic emissions I_{pcc} and therefore V_{pcc} are a combination of primary and secondary emissions. At the turbine terminal marked in red in Fig. 4, the primary emission is the emission from the turbine (I_{p1}) and secondary emission is the emission from the grid background, $I_{grid} = -(I_{pcc} - I_{p1} + \frac{V_{pcc}}{Z_{T1}})$. By applying Kirchhoff's

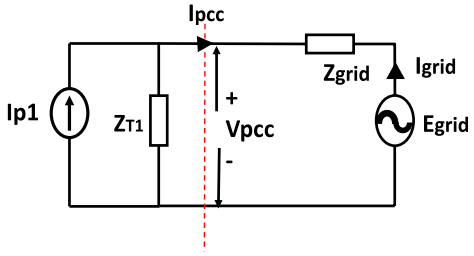

FIGURE 4. A simple mathematical model of a turbine connected to the grid.

current law (KCL) and superposition principle, V_{pcc} and I_{pcc} are equated as in (1), (2) where known variables are I_{pcc}, V_{pcc} from installed power quality meter and Z_{grid} realistic value was obtained from the network owner. Z_{T1}, the turbine impedance and I_{p1} are unknown variables.

$$V_{pcc} = \frac{Z_{T1}}{Z_{T1} + Z_{grid}} * E_{grid} \frac{Z_{T1} * Z_{grid}}{Z_{T1} + Z_{grid}} * I_{p1} \tag{1}$$

$$I_{pcc} = \frac{-1}{Z_{T1} + Z_{grid}} * E_{grid} \frac{Z_{T1}}{Z_{T1} + Z_{grid}} * I_{p1} \tag{2}$$

(1), (2) can be reformulated in the matrix form as

$$\begin{bmatrix} Z_{grid} & -(V_{pcc} - E_{grid}) \\ 1 & -I_{pcc} \end{bmatrix} * \begin{bmatrix} x \\ y \end{bmatrix} = \begin{bmatrix} Z_{grid} * V_{pcc} \\ Z_{grid} * I_{pcc} + E_s \end{bmatrix} \tag{3}$$

where $x = I_{pcc}\, Z_{T1},\ y = Z_{T1}$

Equation (3) represents a mathematically underdetermined system and neither I_{p1} or Z_{T1} can be solved as:

$$Det, \Delta = -Z_{grid} I_{pcc} + V_{pcc} - E_{grid} = 0 \tag{4}$$

Therefore, it was concluded that harmonic contribution estimation in a system with a single turbine and grid is impossible mathematically. There exist 2 equations and 4 unknowns. The same concept was further extended to a system with multiple turbines operating together with the grid as in Fig. 5 and analyzed mathematically. The aim was to investigate the feasibility of a solution to the problem with measurements of current and voltage at multiple locations in a multi-turbine operating system (to check if there was a

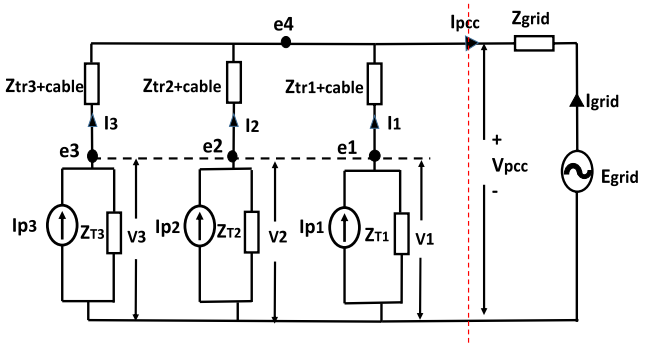

FIGURE 5. A mathematical model of three turbines connected to the grid.

possibility to have equal no. of equations and unknowns), i.e. if Z_{T1} and I_{p1} can be determined through measurements.

The entire system can be represented by the node admittance matrix as in (5):

$$\begin{bmatrix} Ip1 \\ Ip2 \\ Ip3 \\ I_{grid} \end{bmatrix} = \begin{bmatrix} Y_{T1}+a & 0 & 0 & -a \\ 0 & Y_{T2}+b & 0 & -b \\ 0 & 0 & Y_{T3}+c & -c \\ -a & -b & -c & Y_{grid}+a+b+c \end{bmatrix} * \begin{bmatrix} e_1 \\ e_2 \\ e_3 \\ e_4 \end{bmatrix} \quad (5)$$

where $a = Y_{tr1+cable1}, b = Y_{tr2+cable2}, c = Y_{tr3+cable3}$ are the corresponding transformer plus cable impedances. The known variables are $e_1 = V_1$, $e_2 = V_2$, $e_3 = V_3$, from power quality monitors at 400 V, $e_4 = V_{pcc}$ from the power quality monitor at 10 kV, I_{grid} the Norton equivalent current of E_{grid} which is the background grid emission, $Y_{tr+cable}$ the transformer plus cable impedance. The unknown variables are the primary emissions from individual turbines I_{p1}, I_{p2}, I_{p3}, the corresponding turbine impedances Z_{T1}, Z_{T2}, Z_{T3} and the background/ secondary emission I_{grid}.

In (5), there are six unknowns with only three linear equations and hence still underdetermined. Even if assumed that all the turbines have the same impedance ($Z_{T1} = Z_{T2} = Z_{T3} = Z$), there are four unknowns and three equations. It was verified that the equation in the last row of the matrix is redundant (contains only known variables) and does not add any additional information to solve the system. Therefore, even with multiple location measurements, there is no solution to the harmonic contribution estimation problem. With additional assumption $I_{p1} = I_{p2} = I_{p3}$ the equations can be solved but due to the dynamic behavior of the emission from each turbine (or the system), this condition is seldom met from our practical experience. From the above analysis, it can be inferred ($I_p.Z_T$) is a coupled term and knowledge of the turbine dynamic impedance is necessary to have a deterministic solution mathematically. It was also understood that performing measurements at multiple locations in a wind park narrows down to the same single turbine case without having assumptions that are seldom met in reality.

IV. INFERENCES FROM ANALYSIS OF FIELD MEASUREMENTS

This section presents the analysis of field measurements. Three different scenarios of turbine operation to show the behavior of harmonics at the individual turbine terminal and a scenario at the aggregation point are illustrated. We introduce a new concept of analysis with 'harmonic break-even point', $P_{break-even}$. It helps in identifying whether primary emission or secondary emission dominates (has the highest

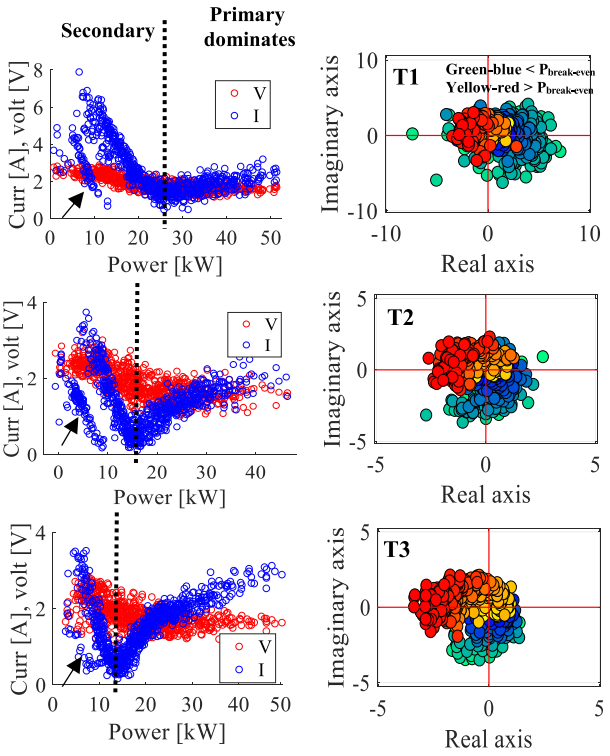

FIGURE 6. 5th harmonic current and voltage at turbine terminal plotted w.r.t power (left column); Complex plot of harmonic current (right column). Note the differences in harmonic magnitude between the three turbines.

responsibility) at the analysis point in the considered period. In Fig. 6-8, the first column represents harmonic current in blue and harmonic voltage in red plotted w.r.t power, the second column represents the complex plot of harmonic current. Harmonic amplitude and phase angles are calculated using interpolated Fast Fourier Transform algorithm. The measurements at turbine terminals T1-T3 are marked in figures.

A. ANALYSIS OF MEASUREMENTS AT THE TURBINE TERMINALS ON A DAY WITH DISTINCT OPERATION OF EACH TURBINE

This is one of the cases where the three turbines were with power production varying between 0 and 50 kW in a period of six hours but operating with individual distinct power and harmonic characteristics. Analysis at the turbine terminal refers to the primary emission to emissions from the turbine and secondary emission to emissions from the upstream grid and other turbines. From the 5th, 7th, 11th, and 13th harmonic characteristics in Fig. 6-8, it was verified that the harmonic emissions do not remain constant w.r.t active power. A cancellation effect at a particular power level is visible in all the cases and is pointed out in all the figures with a vertical dashed line. It was verified that this harmonic cancellation point is different for different turbines and different harmonic orders. This point where harmonic cancellation occurs is termed as 'harmonic break-even point'. It is defined as the point in time where the phase angle of the primary emission

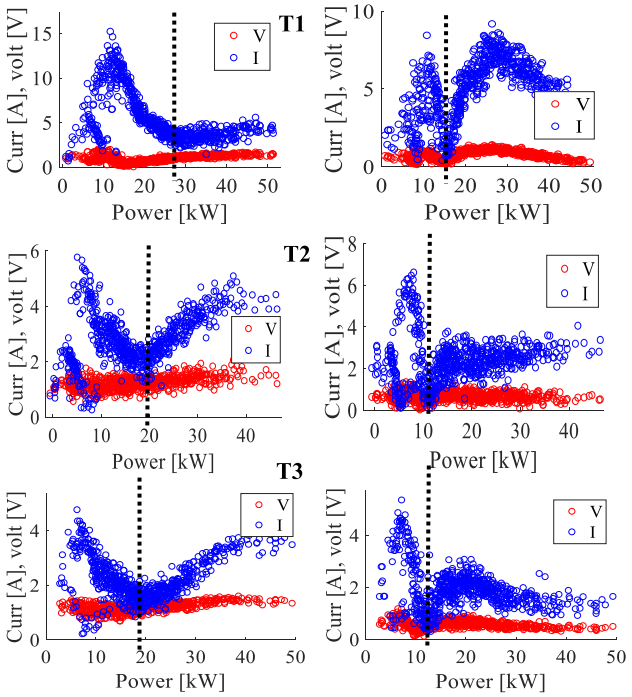

FIGURE 7. 11th harmonic (left column), 13th harmonic (right column) current and voltage at turbine terminal plotted w.r.t power.

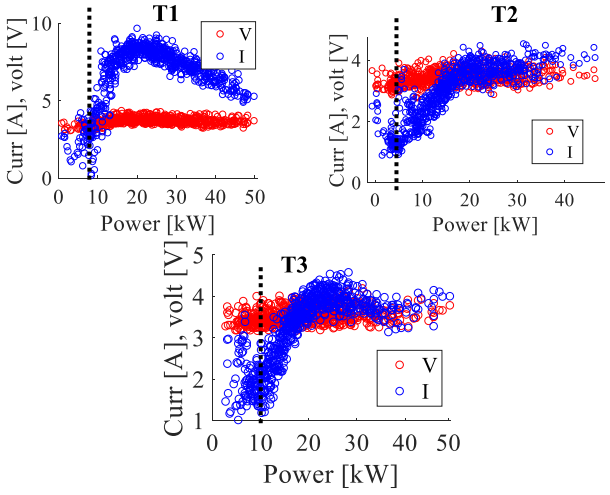

FIGURE 8. 7th harmonic current and voltage at turbine terminal plotted w.r.t power.

and the secondary emission lies in opposite quadrants, i.e. are 180° apart. As the secondary emission originating from neighboring turbines or the upstream grid is not constant with respect to time, this break-even point cannot be predicted based on the production level of the turbine of interest. The break-even point will also not occur for all harmonics at the same time or production level.

The complex plots in Fig. 6 have further re-confirmed the cancellation effect. The complex plot is a complete representation as it includes magnitude and phase angle information (w.r.t fundamental voltage). The increase in color intensity in all the complex plots from green to blue represents measurements below $P_{break-even}$ and from yellow to red represents measurements after $P_{break-even}$. The propagation of complex harmonic currents to the origin at the $P_{break-even}$ confirms the phase angle cancellation effect of harmonic currents from different sources.

It was also important to understand whether the emission from the turbine (primary) or that from the upstream grid and other turbines (secondary) dominates before and after $P_{break-even}$. For this, we focus on the region just before $P_{break-even}$, where two parallel distinct patterns of harmonic current between 0 and 12 kW are visible for 5th, 11th and 13th harmonics in Fig. 6, 7.

It was verified that the pattern to the extreme left (pointed out with arrow in Fig. 6 and visible in Fig. 7) consists of measurements all belonging to the same date and is observed even at the aggregation point of the wind park and at the three turbine terminals at the same day. The appearance of these distinct patterns at the same instant at the aggregation point of the wind park; the eventual cancellation effect at $P_{break-even}$ that follows soon after when power production increases; and the non-appearance of such distinct harmonic pattern during every other instance of turbine operation with the same power production levels leads to the inference that it is not just caused by turbine converter and its associated control system alone. It was inferred that in the region before $P_{break-even}$, secondary emission dominates as the wind power production is low whereas in the region after the $P_{break-even}$, primary emission dominates until the amplitude levels are with the increasing trend due to the increase in power production. Although secondary emission here consists of emissions from the upstream grid together with those resulting from other turbines, the reason for the distinct pattern before $P_{break-even}$ was verified to be due to changes in the upstream grid emissions and was observed only on certain days. Thus, one could conclude that secondary emission dominates primary before $P_{break-even}$. It was also observed from Fig. 6 that T1 has the highest secondary emissions. This is expected as T1 is the closest in distance to the upstream grid as also depicted in the mathematical model in Fig. 5. The observations w.r.t aggregation point of the park is discussed in detail in the forthcoming section.

TABLE 1. $P_{break-even}$, Case: A.

Harmonic	T1	T2	T3
5th, $P_{break-even}$	26 kW	16 kW	13 kW
7th, $P_{break-even}$	10 kW	5 kW	10 kW
11th, $P_{break-even}$	28 kW	20 kW	18 kW
13th, $P_{break-even}$	16 kW	11 kW	12 kW

The $P_{break-even}$ in all the observed cases is between 5 kW and 30 kW as tabulated in Table 1. The harmonic voltage showed lesser variations compared to harmonic current w.r.t the active power. The complex plot to show its variation is shown for the 5th and 7th harmonic in Fig. 9 where the net cancellation effect is not evident compared to harmonic current.

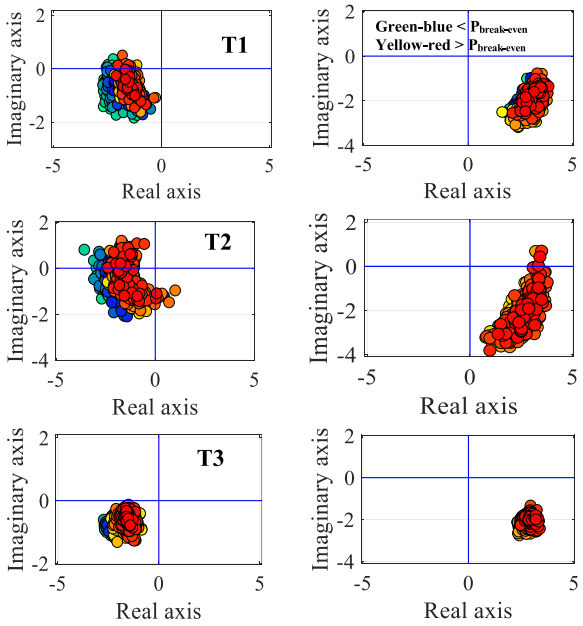

FIGURE 9. 5th (left column), 7th harmonic voltage (right column) complex plot.

B. ANALYSIS OF MEASUREMENTS AT THE AGGREGATION POINT FOR THE SAME PERIOD

At the point where the park is connected to the upstream grid, i.e. the aggregation point, the primary emission is considered as the emission from the wind park as a whole and the secondary emission is the emission from the upstream grid alone. The harmonic current characteristics at the aggregation point for the same period as in the previous scenario are illustrated in Fig. 10. Two distinct parallel patterns of harmonic current before $P_{break-even}$ can be verified at the aggregation point for 5^{th}, 11^{th} and 13^{th} harmonics similar to what is observed at the individual turbine terminal at the same time instant. $P_{break-even}$ at the aggregation point is ≤ 50 kW for all the harmonics (corresponding to about 8.3% of installed production, 1Φ) as in Table 2.

TABLE 2. $P_{break-even}$, Case: B.

Harmonic	Aggregation point
5^{th}, $P_{break-even}$	48 kW
7^{th}, $P_{break-even}$	18 kW
11^{th}, $P_{break-even}$	50 kW
13^{th}, $P_{break-even}$	48 kW

The inference that secondary emission from the upstream grid dominates before $P_{break-even}$ and the primary emission from the wind park dominates after $P_{break-even}$ be validated through the following observations:

1) Two distinct parallel patterns of 5^{th}, 11^{th}, and 13^{th} harmonics seen before $P_{break-even}$ at the individual turbine terminals and aggregation point (marked with an arrow in Fig. 6, 10 and discussed before), despite the individual distinct power characteristics of turbines w.r.t time. Such a parallel pattern is not seen for 7^{th} harmonic in this particular case at individual turbine terminal and aggregation point due to the absence of its variation in the upstream grid.

2) These two distinct patterns were not observed every day (e.g. on the day corresponding to Fig. 11) even with low power production levels which point to that the source of it is not the turbine converter operation alone.

3) The cancellation effect marked by $P_{break-even}$ and visible in the complex plot doesn't appear if only primary emission due to turbine operation alone dominates throughout, nor would it if primary and secondary are in phase, regardless of which one dominates.

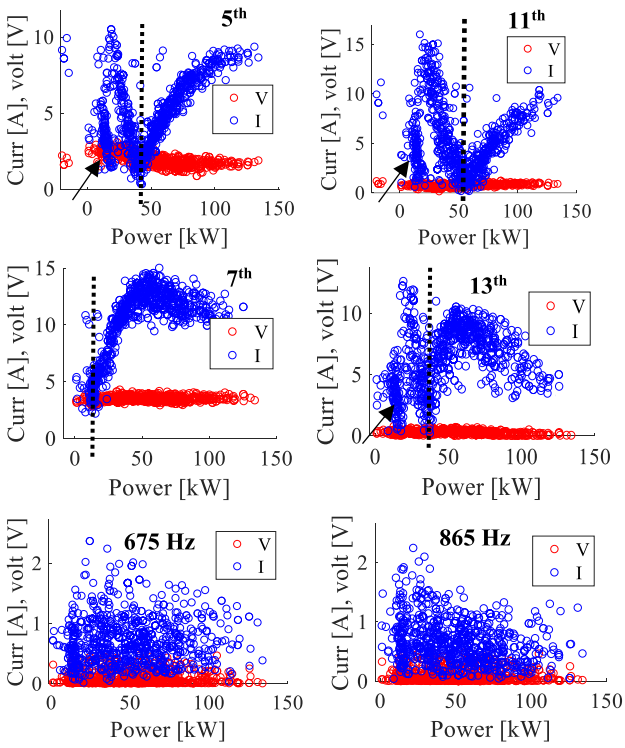

FIGURE 10. Harmonic and interharmonic current and voltage at the aggregation point plotted w.r.t power. The low voltage levels are as a result of measurements at the MV side transformed to the LV side.

The inference that $P_{break-even}$ is the result of the harmonic interaction phenomenon between primary and secondary emission is a result of the following observations and is validated in forthcoming sections.

1) Multiple $P_{break-even}$ didn't exist for the full span of turbine operation. It appears only at the point of vectorial cancellation of harmonic emissions and appears at different power production levels. Therefore, it is not solely dependent on the dynamic converter behavior of the turbine.

2) No $P_{break-even}$ is observed for interharmonic emissions as seen in Fig. 12 due to the absence of interharmonic emissions from the upstream grid. Additionally, if the source is the same and had been the turbine converter,

$P_{break-even}$ should most likely be seen in both harmonic and interharmonic emissions which is not the case here.

3) No $P_{break-even}$ is observed for zero power production of the turbine i.e. load connected is visible then as upstream grid emissions dominates throughout and wind power production is nil.

C. ANALYSIS OF MEASUREMENT AT TURBINE TERMINALS WITH ALL THE TURBINES IN THE FULL SPAN OF OPERATION

A third case is illustrated where all the three turbine operations are alike and achieve a full span of operation from zero to maximum power per phase in six hours.

It was observed that the $P_{break-even}$ exists only once and varies between 5 kW and 30 kW as in Table 3. Another observation is that there is an increased harmonic current distortion during the turbine maximum power operation as seen in Fig. 11. This could be due to an increased converter activity there and is visible as primary emission dominates in this region. This increase in harmonic emission is seen starting at the rated power production level per phase, i.e. 222 kW, at all three turbines irrespective of the time of the day.

TABLE 3. $P_{break-even}$, Case: C.

Harmonic	T1	T2	T3
5^{th}, $P_{break-even}$	20 kW	18 kW	15 kW
7^{th}, $P_{break-even}$	20 kW	5 kW	20 kW
11^{th}, $P_{break-even}$	30 kW	25 kW	25 kW
13^{th}, $P_{break-even}$	13 kW	9 kW	10 kW

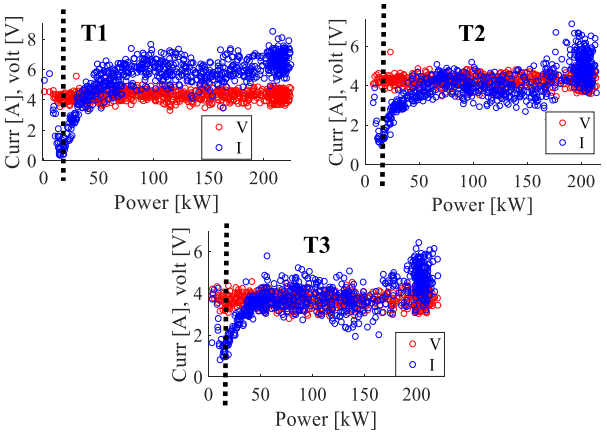

FIGURE 11. 5^{th} harmonic current and voltage at turbine terminal plotted w.r.t power.

To verify the harmonic interaction phenomenon, interharmonics at different frequencies were also plotted against active power and two examples are shown in Fig. 12, row 1. It was observed that there exists no break-even point in the different interharmonic characteristics. This is expected as there is no interharmonic background emission. For 575 Hz, the magnitude almost increases with power. For 855 Hz, the magnitude at 10 kW is comparable to the magnitudes at 150 kW. Row 2 in Fig. 12 shows interharmonic voltage versus

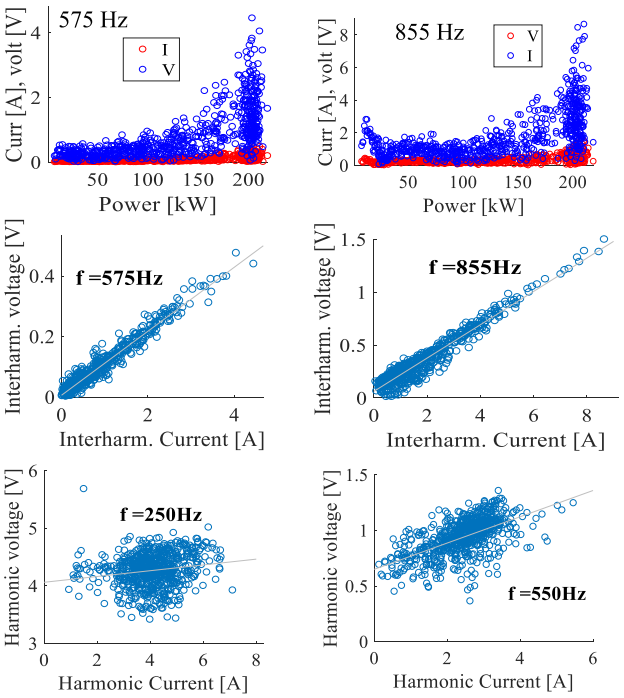

FIGURE 12. Row1: 575 Hz, 855 Hz interharmonics at turbine T3 terminal plotted w.r.t power, Row 2: interharmonic voltage versus interharmonic current, and row 3: harmonic voltage versus harmonic current at turbine terminal.

interharmonic current as a straight line from origin indicating that these are most likely primary emissions from the turbine. This is significantly different from the harmonic plots in row 3 indicating that these measurements are a combination of primary and secondary emissions.

D. ANALYSIS OF MEASUREMENT AT TWO OTHER TURBINES WITH POSITIVE POWER GENERATION AND AT A TURBINE TERMINAL WITH CONNECTED LOAD VISIBLE

A final scenario is illustrated here where one of the turbines, T2, has zero power production and a single-phase load connected is visible in 6 hours. It can be inferred from row 3 of Fig. 13 that the load connected at T2 doesn't exhibit any kind of power-dependent harmonic interaction with the background emissions. The load harmonic current and voltage characteristics appear distributed and constant irrespective of load power variations between 0 and 5 kW. This observation again re-establishes that the harmonic characteristics are defined by the interaction between background emission levels and power production levels of the individual turbines. The emissions seen at the T2 terminal are a combination of primary emissions (harmonic current drawn by load) and secondary emissions (emissions from the upstream grid and other turbines). The absence of $P_{break-even}$ is because of both primary and secondary emissions act in the same direction with no cancellation effect. It is difficult to draw conclusions here which one dominates and has the highest contribution. $P_{break-even}$ for T1, T3 are tabulated in Table 4.

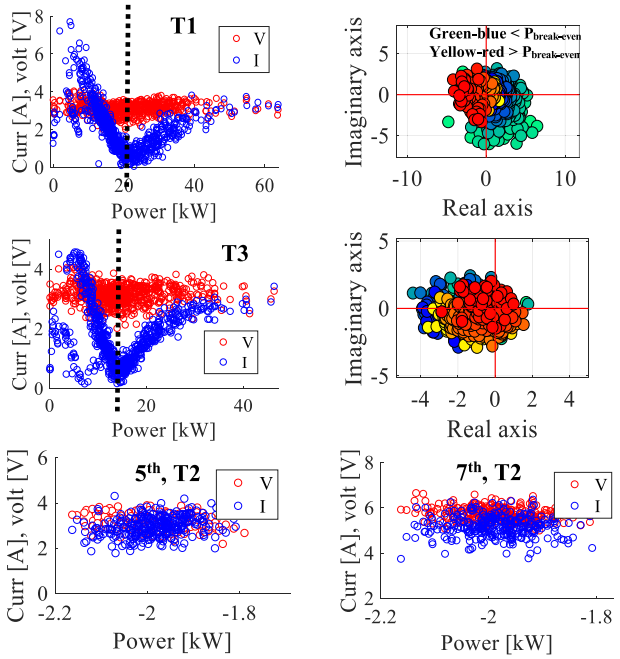

FIGURE 13. 5th harmonic w.r.t power and complex plot of harmonic current at T1, T3 terminal, 5th, and 7th harmonic characteristics of load at T2 terminal.

TABLE 4. $P_{break-even}$, Case: D.

Harmonic	T1	T2	T3
5th, P break-even	20 kW	15 kW	-
7th, P break-even	20 kW	10 kW	-
11th, P break-even	10 kW	9 kW	-
13th, P break-even	16 kW	13 kW	-

V. DISCUSSIONS

Real-life measurements are always a combination of primary and secondary emission at any point in time. The objective to distinguish between primary and secondary emissions was to estimate harmonic contributions from respective sources. From the mathematical analysis, it is proven that this is impossible unless known the individual dynamic turbine impedances. It was also verified that the distinction is impossible even with multiple measuring points in a wind park. Even though the theoretical modeling approach is simple, it supports and proves the fact that by measurements alone the sharing of emissions from each turbine as well as background emission cannot be determined. The harmonic voltage versus harmonic current plots also failed to provide any information about the turbine impedances (slope not defined). Therefore, the exact percentage share of harmonics from the interacting sources at any point in a wind park cannot be estimated just by performing field measurements.

A second objective was to evaluate which source has the highest responsibility/contribution at an instant. An in-depth analysis of field measurements was done to investigate how much information one can get to get closer to a solution. It was found that the individual harmonic characteristic is defined by the harmonic interaction phenomenon which depends on the time-varying background distortion levels and operating power levels of turbines and wind park.

A new concept of the 'harmonic interaction break-even point' was introduced with the help of which, the region where primary emission or secondary emission dominates can be pointed out. For example, at the aggregation point whether the percentage share of utility is more or that of the wind park is more at any instant can be stated. In this particular wind park, it can be stated that at the aggregation point when the power production levels are less than 50 kW ($<$ 8% of the per phase power production), it is the utility that has the highest responsibility towards total harmonic distortion (THD). And when the power production levels are greater than 50 kW it is the wind park owner that has the highest responsibility towards THD. This conclusion is drawn with respect to the observations from most of the analysed cases. It is worth mentioning here that there were exceptions to this conclusion where in some cases after the $P_{break-even}$ point and after an increasing trend in harmonic amplitude levels, a reduction in amplitude levels of harmonics is also observed. This could be due to the time-varying and increased levels of secondary emissions. Whereas for interharmonics, as there exists no interharmonic interaction mechanism, the dependency of interharmonics solely on the power production levels of turbines/park can be established. This means that the wind park owner is solely responsible for the interharmonic emissions.

A third objective to understand the time-varying nature of primary and secondary emissions is possible with the help of $P_{break-even}$. For example, at the turbine terminal, $P_{break-even}$ is varying between 5-30 kW ($<$ 14% of the per phase power production) and at the aggregation point, $P_{break-even}$ is varying between 18-50 kW ($<$ 8% of the per phase power production).

From long-term measurements, one can thus define a magnitude of production where a certain harmonic order is canceled (or reaches its lowest magnitude). The magnitude of production where this occurs will vary with the secondary emissions. If one finds this cancellation point, one can define a level of secondary/primary/primary + secondary emission (or at least a feasible range).

Considering an example of 5th harmonic in Fig. 6 at the turbine terminal and Fig. 10 at the aggregation point, the estimated feasible ranges of secondary (at around nil power production) and primary emission levels (at max. power) are tabulated in Table 5. After the cancellation point ($P_{break-even}$) the feasible primary emission levels should be at least double the values to attain the observed magnitude levels in Fig. 6, 10 (considering phase opposition between primary and secondary and negligible variations in secondary emission levels). This input of plausible levels of primary/secondary emission can be used in (5) in the estimation of turbine impedance values at that particular harmonic. It is represented in the last column, Table 5. As estimation of impedances is not the primary objective of this paper, thus we represent only one illustrative example.

TABLE 5. An example for feasible ranges of 5th harmonic emissions and impedances.

Analysis point	Secondary Emission (A)	Primary Emission (A)	Harmonic voltage (V)
Turbine, T1	4 – 8	7 – 11	$e_1 = 2$
Turbine, T2	2 – 4	4 – 6	$e_2 = 2$
Turbine, T3	2 – 4	5 – 7	$e_3 = 2$
Aggregation point	3 – 11	13 – 20	$E_{grid} = 1.8$
Estimated turbine impedance range (Ω)	$Z_{T1} = 4 - 6$; $Z_{T2} = 2 - 3$; $Z_{T3} = 3 - 4$		

From the observed primary/secondary emission levels for different harmonics, one can conclude that the values are different of the three turbines in all the cases and therefore the dynamic turbine impedances, even though they are from identical manufacturer. This again re-establishes the fact that one cannot make equality assumptions in the mathematical model for finding the solution for harmonic contribution. It can be thus inferred that neither the simulation model nor the measurements should be considered independently to derive conclusions. The inferences from measurements helps to validate the assumptions in our model. Thus a combination of both is preferred in harmonic assessment especially in distributed energy generation with non-steady state operation.

From our practical experience, 60 to 70% of the time wind park operates in the region as marked in Fig. 14 which represents the operating characteristics of a turbine within a downward transcend of power production from max power to negative power (load connected visible). The rest 30% of the time wind park operation is either around maximum power or around nil power (increased converter activity) with increased waveform distortions. It can be stated from Fig. 6-13, that within the 60 to 70% operation time the interaction between background emissions and primary emissions from turbines/park actually lowers the harmonic magnitude levels. Whereas at around nil production and maximum production the individual harmonic magnitude levels are almost comparable for many cases.

The authors are very well aware of the fact that the interferences w.r.t harmonic interactions are highly system-dependent but at least the feasibility of the proposed method is to be investigated irrespective of the difference in systems to approximately estimate the background and source emission levels with long-term measurements. Long-term measurements of the background emission (magnitude, phase angle, and likely range of variation) should be included in decisions on permitted harmonic levels for the connection of wind parks. For simulation studies, one has to consider uncertainties related to background emissions and the same thing with studies based on measurements. It has to be identified which one has lower uncertainty and whether combining the two leads to less uncertainty, but a validation of either is not straightforward.

This study is based on a specific three-turbine system and further studies are needed for understanding of generalized use of the results. The practicability of the proposed method is based on the availability of long-term measurements, and a statistical analysis approach generating knowledge on the relation between already known harmonic cancellation phenomenon and power production levels of the wind turbines/wind park. This paper has not considered any possible resonance and non-linear interactions in the illustrated cases and analysis. It is also worth mentioning that the main resonance frequencies identified at different analysis points in this network were at higher frequencies greater than 13th harmonic.

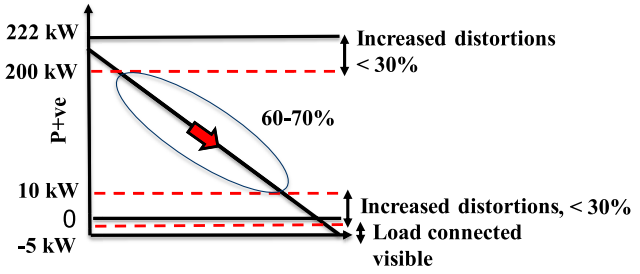

FIGURE 14. Single phase operating characteristics of a turbine.

VI. CONCLUSION

This paper contributes to the existing knowledge of harmonic interaction mechanisms in a wind park and investigates the feasibility to find a solution to harmonic contribution estimation in a wind park with limited information available. With the analysis of long-term measurements using the proposed concept, the feasible background emission levels and emissions from wind park can be estimated. Even though multiple methods are proposed in the literature to solve the yet challenging harmonic contribution estimation problem the practicability of these methods is still a question. As harmonic levels at any given point in the park vary with time, through this work we discuss a practical way of harmonic assessment combining the inferences from simulation models with reality in the search for a practical solution. This novel concept of harmonic analysis must be investigated in a larger-scale onshore/offshore wind park with a large no. of turbines where actually issues due to harmonic interactions and harmonic amplification due to resonances find prominence.

REFERENCES

[1] D. Horning. (Nov. 2014). *White Paper: Steps to Find the Source of Harmonics*. [Online]. Available: http://library.powermonitors.com
[2] I. Papic, D. Matvoz, A. Spelko, W. Xu, Y. Wang, D. Mueller, C. Miller, P. F. Ribeiro, R. Langella, and A. Testa, "A benchmark test system to evaluate methods of harmonic contribution determination," *IEEE Trans. Power Del.*, vol. 34, no. 1, pp. 23–31, Feb. 2019.
[3] K. Srinivasan and R. Jutras, "Conforming and non-conforming current for attributing steady-state power quality problems," *IEEE Trans. Power Del.*, vol. 13, no. 1, pp. 212–217, Jan. 1998.
[4] C. Chen, X. Liu, D. Koval, W. Xu, and T. Tayjasanant, "Critical impedance method—A new detecting harmonic sources method in distribution systems," *IEEE Trans. Power Del.*, vol. 19, no. 1, pp. 288–297, Jan. 2004.
[5] T. Tanaka and H. Akagi, "A new method of harmonic power detection based on the instantaneous active power in three-phase circuits," *IEEE Trans. Power Del.*, vol. 10, no. 4, pp. 1737–1742, Oct. 1995.

[6] S. T. Tentzerakis and S. A. Papathanassiou, "An investigation of the harmonic emissions of wind turbines," *IEEE Trans. Energy Convers.*, vol. 22, no. 1, pp. 150–158, Mar. 2007.
[7] S. Liang, Q. Hu, and W.-J. Lee, "A survey of harmonic emissions of a commercially operated wind farm," *IEEE Trans. Ind. Appl.*, vol. 48, no. 3, pp. 1115–1123, May 2012.
[8] J. Plotkin, V. Petrushin, and M. Reichwald, "Harmonic current pollution source determination in a grid connected wind farm," in *Proc. 17th Eur. Conf. Power Electron. Appl. (EPE ECCE-Europe)*, Geneva, Switzerland, Sep. 2015, pp. 1–5.
[9] B. Badrzadeh and M. Gupta, "Practical experiences and mitigation methods of harmonics in wind power plants," *IEEE Trans. Ind. Appl.*, vol. 49, no. 5, pp. 2279–2289, Sep. 2013.
[10] A. M. Blanco, B. Heimbach, B. Wartmann, J. Meyer, M. Mangani, and M. Oeschger, "Harmonic, interharmonic and supraharmonic characterisation of a 12 MW wind park based on field measurements," *CIRED-Open Access Proc. J.*, vol. 2017, no. 1, pp. 677–681, Oct. 2017.
[11] M. H. J. Bollen and S. K. Rönnberg, "Primary and secondary harmonics emission; harmonic interaction—A set of definitions," in *Proc. 17th Int. Conf. Harmon. Qual. Power (ICHQP)*, Belo Horizonte, Brazil, Oct. 2016, pp. 703–708.
[12] K. Yang, "On harmonic emission, propagation and aggregation in wind power plants," Ph.D. dissertation, Dept. Electr. Power Eng., Luleå Tekniska Universitet, Luleå, Sweden, 2015.
[13] I. N. Santos, J. C. Oliveira, P. F. Ribeiro, A. Reis, A. C. Santos, and I. N. Gondim, "Applying the superposition procedure for the harmonic sharing responsibility between renewable energy power plants and the network," *Int. J. Emerg. Electr. Power Syst.*, vol. 15, no. 3, pp. 237–246, Jun. 2014.
[14] *Wind Energy Generation Systems—Part 21-3: Measurement and Assessment of Electrical Characteristics—Wind turbine harmonic model and its application*, document IEC TR 61400-21-3, Ed.1, 2019.
[15] J. Arrillaga, N. R. Watson, and S. Chen, "Power quality monitoring," in *Power System Quality Assessment*, Hoboken, NJ, USA: Wiley, 2000.
[16] L. Sainz, L. Monjo, J. Pedra, M. Cheah-Mane, J. Liang, and O. Gomis-Bellmunt, "Effect of wind turbine converter control on wind power plant harmonic response and resonances," *IET Electr. Power Appl.*, vol. 11, no. 2, pp. 157–168, Feb. 2017.

VINEETHA RAVINDRAN (Student Member, IEEE) received the M.Tech. degree in power electronics and electric drives from the National Institute of Technology, Surat, India, in 2012. She is currently pursuing the Ph.D. degree with Luleå Technical University, Skellefteå, Sweden. Her research interests include power electronics and electric drives, power quality, signal processing, and embedded systems.

NASER NAKHODCHI (Graduate Student Member, IEEE) received the B.Sc. degree from the Ferdowsi University of Mashhad, Iran, and the M.Sc. degree from the University of Skövde, Sweden. He is currently pursuing the Ph.D. degree with the Department of Engineering Sciences and Mathematics, Luleå University of Technology, Sweden. His research interests include power quality and renewable energy systems.

SARAH RÖNNBERG (Senior Member, IEEE) received the Ph.D. degree in electrical power engineering from the Luleå University of Technology, Skellefteå, Sweden, in 2013. She is currently an Associate Professor with the Department of Engineering Sciences and Mathematics, Luleå University of Technology. Her research interests include supraharmonics, power systems harmonics, and power quality in general.

MATH H. J. BOLLEN (Fellow, IEEE) received the M.Sc. and Ph.D. degrees from the Eindhoven University of Technology, Eindhoven, The Netherlands, in 1985 and 1989, respectively. He has been a Lecturer with the University of Manchester Institute of Science and Technology (UMIST), Manchester, U.K.; a Professor of electric power systems with the Chalmers University of Technology, Gothenburg, Sweden; a Research and Development Manager, and the Technical Manager of power quality and distributed generation with STRI AB, Gothenburg; and a Technical Expert with the Energy Markets Inspectorate, Eskilstuna, Sweden. He is currently a Professor of electric power engineering with the Luleå University of Technology, Skellefteå, Sweden. He has authored or coauthored a few 100 articles including a number of fundamental articles on voltage dip analysis, two textbooks on power quality, such as *Understanding Power Quality Problems* and *Signal Processing of Power Quality Disturbances*, and two textbooks on the future power systems, such as *Integration of Distributed Generation in the Power System* and *The Smart Grid—Adapting the Power System to New Challenges*. He has defined voltage dips as a research subject, has spread the use of the term hosting capacity, and has contributed to defining supraharmonics as a research area. He was a recipient of the CIGRE Study Committee Award.